

# Formation and Destiny of White Dwarf and Be Star Binaries

Chun-Hua Zhu<sup>1</sup>, Guo-Liang Lü<sup>1,2</sup>, Xi-Zhen Lu<sup>1</sup>, and Jie He<sup>1</sup>

School of Physical Science and Technology, Xinjiang University, Urumqi 830046, China; chunhuazhu@sina.cn

<sup>2</sup> Xinjiang Astronomical Observatory, Chinese Academy of Sciences, Urumqi 830011, China

Received 2022 September 15; revised 2022 December 27; accepted 2022 December 28; published 2023 January 31

#### Abstract

The binary systems consisting of a Be star and a white dwarf (BeWDs) are very interesting. They can originate from the binaries composed of a Be star and a subdwarf O or B star (BesdOBs), and they can merge into red giants via luminous red nova or can evolve into double WD potentially detected by the LISA mission. Using the method of population synthesis, we investigate the formation and the destiny of BeWDs, and discuss the effects of the metallicity (Z) and the common envelope evolution parameters. We find that BesdOBs are significant progenitors of BeWDs. About 30% (Z = 0.0001) –50% (Z = 0.02) of BeWDs come from BesdOBs. About 60% (Z = 0.0001) –70% (Z = 0.02) of BeWDs turn into red giants via a merger between a WD and a non-degenerated star. About 30% (Z = 0.0001) –40% (Z = 0.02) of BeWDs evolve into double WDs which are potential gravitational waves of the LISA mission at a frequency band between about  $3 \times 10^{-3}$  and  $3 \times 10^{-2}$  Hz. The common envelope evolution parameter introduces an uncertainty with a factor of about 1.3 on BeWD populations in our simulations.

Key words: (stars:) binaries (including multiple): close - stars: evolution - stars: rotation - (stars:) white dwarfs

#### 1. Introduction

High mass X-ray binaries (HMXBs) consist of a massive star and a compact object, in which the massive star may be a red supergiant star or a Be star, and the compact object may be a black hole or a neutron star (NS). There are about more than 240 HMXBs observed in the galaxy and the Magellanic Clouds (MCs) (Liu et al. 2005, 2006). The majority of the known HMXBs are composed of Be stars and NSs (BeNSs), which are called as Be/X-ray binaries. Meurs & van den Heuvel (1989) estimated that there should be 2000–20,000 Be/X-ray binaries in the galaxy.

The compact stars in Be/X-ray binaries can also be white dwarfs (WDs). They are marked as BeWDs in this paper. Based on the model of binary evolution, Raguzova (2001) predicted that the number of BeWDs in the galaxy should be 7 times more than that of BeNSs. Unfortunately, there are only seven BeWDs or candidates observed in the MCs, which are listed in Table 1. Compared with BeNSs, the X-ray spectrum produced by BeWDs is very soft, which is absorbed more easily. Especially, due to the much higher extinction rates in the plane of the Milky Way, up to now, no BeWD is known in the galaxy. Beside the above observational biases, Kennea et al. (2021) considered that the metallicity may significantly affect the evolution of BeWDs.

In spite of observational constraints, there should be a large number of BeWDs in the universe. They involve a Be star and an accreting WD. The former has a B-type spectrum, a high rotational velocity and a decretion disk (Porter & Rivinius 2003). The origin of this disk is still unclear. The majority of Be stars are usually produced by binary interaction (e.g., Ablimit & Lü 2013; de Mink et al. 2013; Hastings et al. 2021). Therefore, the progenitor of WD in BeWD transfers enough matter to spin up its companion, even it can lose whole envelope, and becomes a naked helium star. On observations, naked helium star is considered as subdwarf O or B (sdOB) star (Sargent & Searle 1968; Heber 1986; Han et al. 2002). A binary system, consisting of a sdOB star and a Be star, is called as BesdOB. Naze et al. (2022) listed known 25 BesdOB and candidates (Wang et al. 2018, 2021, references therein), which are listed in Table 2. Obviously, it is very interesting to discuss whether these BesdOBs can evolve into BeWDs. The latter is the potential progenitor for type Ia supernova (SN Ia) (e.g., Wang & Han 2012) or millisecond pulsar (MSP) (e.g., D'Antona & Tailo 2020), which depends on accreting compact object being CO WD or ONe WD. In addition, the mass of Be stars is between about 2 and 20  $M_{\odot}$  (Porter & Rivinius 2003). They finally become WDs or NSs. Then, BeWDs evolve into systems consisting of double compact objects which are good gravitational sources detected by the Laser Interferometer Space Antenna (LISA) (Amaro-Seoane et al. 2017; Lü et al. 2020).

There are many theoretical studies for Be binaries, such as Be/X-ray binaries, BesdOBs, BeWDs, and so on (e.g., Raguzova 2001; Shao & Li 2014; Brown et al. 2019; Shao & Li 2021). Especially, Brown et al. (2019) considered the interaction between NS and decretion disk in Be/X-ray binaries. However, this interaction is seldom included in

Table 1
Parameters of the Observed BeWDs

BeWD	$P_{\text{orb}}$ (day) $L_{\text{X}}$ (erg s <sup>-1</sup> )		$M_{ m WD}~(M_{\odot})$	Be star	galaxy	References
XMMU J052016.0-692505	510 or 1020	$10^{34} - 10^{38}$	0.9-1.0	В0-В3е	LMC	K06
XMMU J010147-715550	1264	$\sim 4.4 \times 10^{33}$	1.0	O7IIIe-B0Ie	SMC	S12
MAXI J0158-744	•••	$>10^{37}$ ; $10^{40}$ of peak luminosity	1.35	B1-2IIIe	SMC	L12,M13
SWIFT J011511.0-725611	17.402	$2 \times 10^{33}  3.3 \times 10^{36}$	1.2	O9IIIe	SMC	K21
SWIFT J004427.3734801	21.5	$5.7-2.9 \times 10^{36}$	•••	O9Ve-B2IIIe	SMC	C20
RX J0527.8-6954	•••	$4-9 \times 10^{36}$	•••	B5eV	LMC	O10

Note. Columns 1–7 list the name of BeWDs, orbital period  $P_{\text{orb}}$ , X-ray luminosity, estimated WD's mass, the spectral type of Be star, hosted galaxy and references. References: K06-Kahabka et al. (2006); S12-Sturm et al. (2012); L12-Li et al. (2012); M13-Morii et al. (2013); K21-Kennea et al. (2021); C20-Coe et al. (2020); O10-Oliveira et al. (2010).

 Table 2

 Parameters of the Observed BesdOBs in the Galaxy

BesdOB	$P_{\rm orb}$ (day)	$M_{ m sdOB}~(M_{\odot})$	$T_{\rm eff}$ (kK)(sdOB)	$\log L(L_{\odot})$ (sdOB)	$M_{\mathrm{Be}}~(M_{\odot})$	$T_{\rm eff}~({\rm kK})({\rm Be})$	$\log L(L_{\odot})$ (Be)	References			
V2119 Cyg	63.1	$1.62 \pm 0.28$	43.5	$2.92^{0.15}_{-0.23}$	$8.65 \pm 0.35$	25.6	$3.83 \pm 0.02$	K22			
60 Cyg	147.68	$1.2 \pm 0.2$	42	2.78	$7.3\pm1.1$	27	$3.99 \pm 0.04$	K22			
28 Cyg	246		45	< 2.39		20.47	$3.76\pm0.02$	K22			
o Puppis	28.9							K12			
$\varphi$ Persei	126.67	$1.2 \pm 0.2$	53	$3.79 \pm 0.13$	$9.6 \pm 0.3$	29.3	$4.16\pm0.04$	M15			
HR 2142	80.9	0.7	>43	>1.7	9	21	$4.17\pm0.10$	P16			
59 Cygni	28.2	0.79	52.1	$3.0 \pm 0.1$	7.9	21.8	$4.14\pm0.12$	P13			
FY CMa	37.3	1.26	45	3.38	12.6	27.5	$4.43 \pm 0.03$	P13			
HD 55 606	93.8	0.9	40.9	$2.27^{+0.13}_{-0.19}$	6.2	27.35	$3.60\pm0.03$	C18			
HR 6819	40.335	$0.46 \pm 0.26$	16	$3.12 \pm 0.10$	$7\pm2$	20	$3.77 \pm 0.04$	B20			
$\zeta$ Tau	132.987	0.87-1.02			11	19.3	$3.75 \pm 0.04$	R09			
AlS8775	78.999	1.5	12.7	2.8	$7\pm2$	18	$3.10\pm0.07$	S20			
MX Pup	5.1526	0.6-6.6	•••	•••	15	25.1	$4.24\pm0.03$	C02			
$\chi$ Oph	34.1 or 138.8	3.8	•••	•••	10.9	20.9	$3.75\pm0.02$	A78, H87,T08			
HD 161 306	99.9	0.0567	•••	•••	•••		$3.56\pm0.01$	K14			
V1150 Tau	•••		40	$2.11^{+0.14}_{-0.21}$	•••	20.53	$3.47\pm0.02$	W21			
HR2249			38.2	$2.68^{+0.15}_{-0.23}$	8.5	21.5	$3.55\pm0.02$	W21			
QY Gem			43.5	$2.75^{+0.13}_{-0.18}$		20	$3.49 \pm 0.03$	W21			
V378 Pup			42	$2.83^{+0.14}_{-0.20}$		20	$3.99 \pm 0.03$	W21			
LS Mus			45	$2.82^{+0.23}_{-0.53}$		22.8	$3.86\pm0.03$	W21			
kap01 Aps			40	$2.64_{-0.20}^{+0.14}$		23.95	$3.83 \pm 0.02$	W21			
V846 Ara			42	$2.28^{+0.14}_{-0.21}$		19.8	$3.39 \pm 0.01$	W21			
$\iota$ Ara			33.8	$2.60^{+0.15}_{-0.23}$		25.86	$3.95\pm0.02$	W21			
V750 Ara			45	<2.61		25	$4.49 \pm 0.04$	W21			
8Lac A			45	< 2.71	•••	27.38	$4.17\pm0.05$	W21			

Note. Columns 1–9 list the name of BesdOB, orbital period  $P_{\rm orb}$ , mass, effective temperature and luminosity of sdOB, mass, effective temperature and luminosity of Be star and references. References: K22-Klement et al. (2022); K12-Koubský et al. (2012); M15-Mourard et al. (2015); P13-Peters et al. (2013); P16-Peters et al. (2016); C18-Chojnowski et al. (2018); B20-Bodensteiner et al. (2020); R09-Ruždjak et al. (2009); S20-Shenar et al. (2020); C02-Carrier & Burki (2002); A78-Abt & Levy (1978); H87-Harmanec (1987); T08-Tycner et al. (2008); K14-Koubský et al. (2014); W21-Wang et al. (2021).

BeWDs. In the present paper, we focus on the formation of BeWDs via BesdOBs or other channels, and their destiny (SN Ia or MSP) when WD's mass reaches Chandrasekhar mass by accreting the decretion disk of Be star. In Section 2, the assumptions and some details of the modeling algorithm are given. In Section 3, the properties of the model population of

BeWDs, their formation channel and destiny are presented. Conclusions follow in Section 4.

#### 2. Model

BeWDs' formation and evolutionary involve binary interactions: tidal interaction, mass transfer, common envelope evolution

(CEE), and so on. We use the rapid binary star evolution (BSE) code (Hurley et al. 2002; Kiel & Hurley 2006). In the BSE code, the stellar structure and evolution is described by a serial of fitting formula which depend on the stellar mass, the metallicity and evolutionary age (Hurley et al. 2000). The binary evolution is determined by some binary interactions: mass transfer, tidal interaction, CEE, gravitational radiation, magnetic braking, and coalescence. Among them, the mass transfer, the tidal interaction and the magnetic braking can directly impact on the stellar rotation. These interactions may introduce some uncertain input parameters. If any input parameter is not specially mentioned in the next subsection, it is taken as the default value in these papers.

#### 2.1. Be Star

The mean value of rotational velocities of Be stars is about 70%–90% of the Keplerian critical velocity ( $v_{\rm cr}$ ), and the range of their masses is between 3 and 22  $M_{\odot}$  (Porter & Rivinius 2003; Ekström et al. 2008). Following Ekström et al. (2008), we assume that a main-sequence star becomes Be star when its rotational velocity exceeds 0.7  $v_{\rm cr}$  and its mass is between 3 and 22  $M_{\odot}$ .

The formation of Be star has been investigated by a lot of works (e.g., Ekström et al. 2008; de Mink et al. 2013; Shao & Li 2014, 2021). They meticulously discussed the effects of many uncertain parameters, which include the critical mass ratio  $(q_{\rm cr})$  for dynamically unstable mass transfer, the efficiency of mass accretion when the accretor is spun up to  $v_{\rm cr}$ , the combining parameter  $\lambda \times \alpha_{\rm CE}$  during CEE, the initial mass function, the initial separation and mass, and so on. Considering that BeWDs and their progenitors are located at the MCs or the Milky Way, we take different metallicities ( $Z=0.0001,\ 0.004,\ 0.008$  and 0.02) for different galaxies. In addition, based on the crucial importance of CEE for binary evolution, the effects of combining parameter  $\lambda \times \alpha_{\rm CE}$  on BeWD population are discussed.

# 2.2. Decretion Disk and Mass-loss Rate of Be Star

Because the decretion disk around a Be star is quite complicated, its formation and dynamical evolution is still poorly known (Haubois et al. 2012; Rivinius et al. 2013). Based on a large number of numerical simulations, the decretion disk is fed by material ejected from the Be star, and it diffuses outwards (e.g., Ghoreyshi et al. 2018; Rímulo et al. 2018). The observational evidence and theoretical estimates show that the typical mass of a decretion disk is between  $10^{-8}$  and  $10^{-10}$   $M_{\odot}$  (Vieira et al. 2017; Rímulo et al. 2018). Based on the theoretical simulations of Panoglou et al. (2016); Ghoreyshi et al. (2018), the mass ejection rate from a Be star to its decretion disk is typically about  $10^{-7}$   $M_{\odot}$  yr<sup>-1</sup>, while most of ejected materials lose their angular momentum because of themselves interaction, and are re-accreted by the Be star. The typical mass-loss rate is about  $10^{-9}$   $M_{\odot}$  yr<sup>-1</sup> (Panoglou et al. 2016; Ghoreyshi et al. 2018).

The mass-loss rate of B stars has been theoretically developed by Vink et al. (2000) and Vink et al. (2001), and can be calculated by stellar parameters (luminosity, effective temperature, metallicity). Considering the stellar rotation, Langer (1998) gave the mass-loss rate enhanced by

$$\dot{M}_{\Omega} = \left(\frac{1}{1 - \Omega/\Omega_{cr}}\right)^{\beta} \dot{M}_{0},\tag{1}$$

where  $\dot{M}_0$  is the mass-loss rate calculated by Vink et al. (2001),  $\beta = 0.43$  (Langer 1998),  $\Omega$  and  $\Omega_{\rm cr}$  are the angular velocity and the critical angular velocity, respectively.

The out flow of a Be star consists of a slow equatorial decretion disk and a polar wind (Bogovalov & Petrov 2021). The mass density of decretion disk can be higher than that of polar wind by two orders of magnitude (Bjorkman & Cassinelli 1993). Following Lü et al. (2009), we use aspherical structure to simulate the stellar wind of Be star, and introduce a parameter,  $f_{\rm W}$ , to describe the mass-loss rate via decretion disk:

$$\dot{M}_{\rm disk} = f_{\rm W} \times \dot{M}_{\Omega}.$$
 (2)

Here, if  $f_W = 0$ , there is no decretion disk but a spherical stellar wind; if  $f_W = 0.9$ , there is a decretion disk where 90% mass of stellar wind is in and the left stellar wind is spherical. Considering the density structure of stellar wind from a Be star (Bjorkman & Cassinelli 1993), we take  $f_W = 0.9$  in this work.

For the spherical stellar wind, we use a Bondi & Hoyle (1944) formula to estimate the mass-accretion rate (see details in Hurley et al. 2002). For the decretion disk, there is not an accepted accretion model because it depends on the disk structure, dynamical model and the inclination between the orbital plane and the disk. It is well known that a Be star is misaligned with the orbital plane of BeXB. The main reason is that the binary system experiences an aspherical symmetry supernova when NS is born. However, considering that the progenitors of BeWDs do not undergo violent event like supernova, we assume that the decretion disk is aligned with the orbital plane of BeWD. Therefore, for simplicity, we assume that WD in the BeWDs can accrete all materials in the accretion disk. Of course, we can change  $f_{\rm W}$  value to control the ratio of accreted materials to the matter lost by the Be star.

# 2.3. Method of Population Synthesis

With the help of the method of population synthesis which has been used by a series of papers (Lü et al. 2009, 2012, 2013; Zhu et al. 2015, 2019; Han et al. 2020; Zhu et al. 2021), we simulate the formation and evolution of BeWD's population. The method of population synthesis involves several input parameters: the initial mass function (IMF) of the primaries, the mass-ratio distribution of the binaries and the distribution of initial orbital separations. Following the previous papers, we use the IMF of Miller & Scalo (1979), a constant mass-ratio distribution, and assume a flat distribution over  $1 < \log a_i/R_{\odot} < 6$ , where  $a_i$  is

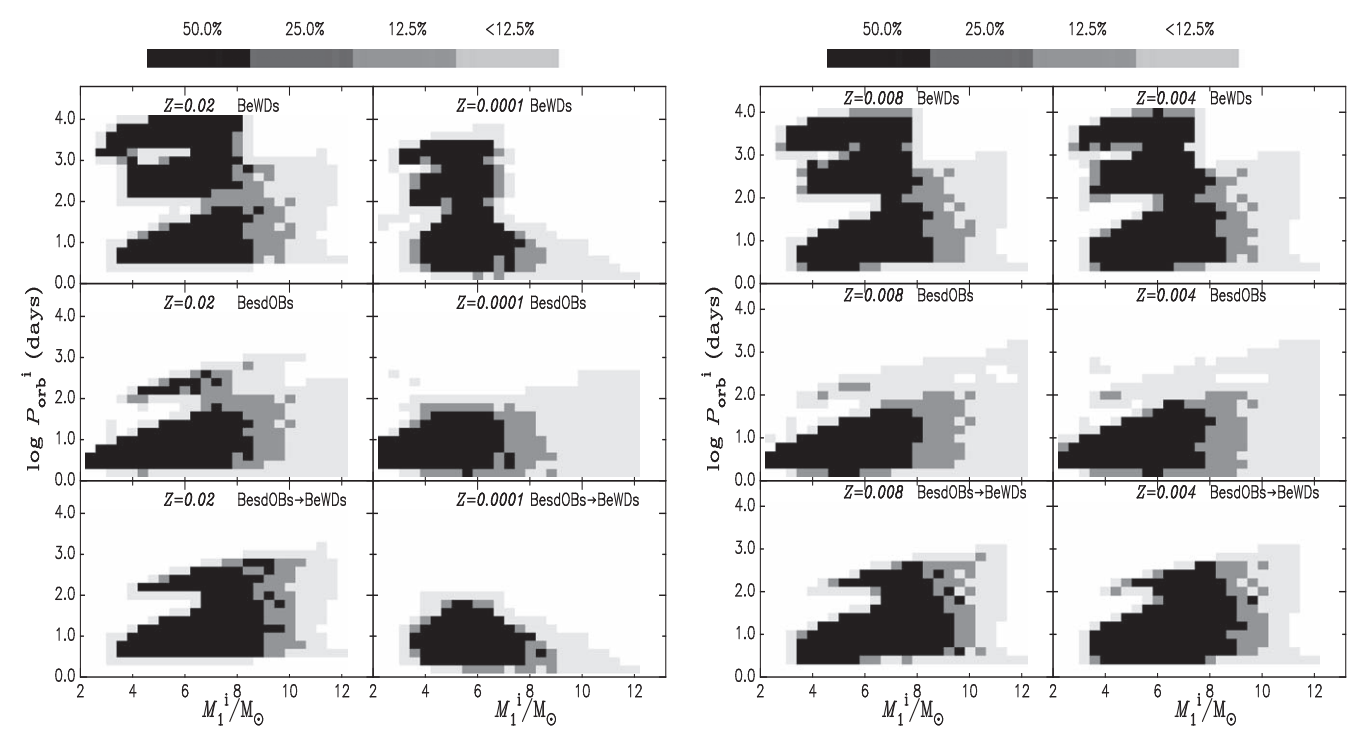


Figure 1. The initial primary masses vs. the initial orbital periods for the progenitors of BeWDs (top panels), BesdOBs (middle panels) and those binaries in which BesdOBs can evolve into BeWDs (bottom panels). Metallicities in different simulations are given in the top-middle zone of each panel.

the initial orbital separation. We take  $10^8$  initial binary systems with initially circular orbits for each simulation. Many input parameters (metallicity, alpha value for the CE, accretion efficiency during mass transfer, the criteria of dynamical mass transfer, etc.) can result in the uncertainties of binary population synthesis (BPS) (Han et al. 2020). For simplicity, we only consider the effects of the metallicity and the CEE on BeWD population in the present paper.

#### 3. Results

As mentioned in the Introduction, the present paper focuses on the formation channel of BeWDs (Especially, the channel from BesdOB), and the destiny of BeWDs in which WDs accrete the materials via Be disk. We calculate  $10^8$  binary evolution with different metallicity ( $Z\!=\!0.0001,\,0.004,\,0.008$  and 0.02) and combining parameters ( $\lambda\times\alpha_{\rm CE}=0.25,\,0.5$  and 1.0). The effects of  $\lambda\times\alpha_{\rm CE}$  is only discussed in the next subsection. If it is not specially mentioned,  $\lambda\times\alpha_{\rm CE}$  is always taken as 0.5.

# 3.1. Progenitors of BeWDs

In all  $10^8$  initial binary systems, about 4.1% (Z=0.02) – 3.7% (Z=0.0001) of them can evolve into BeWDs, and about 4.4%(Z=0.02) -6.2%(Z=0.0001) of them can become BesdOBs. About 33% (Z=0.0001) –51% (Z=0.002) of BesdOBs can evolve into BeWDs. It means that BesdOBs

are the most important progenitors of BeWDs. The average lifetime of BeWDs in our simulations is between about 25 (Z=0.02) and 20 (Z=0.0001) Myr. Following Shao & Li (2014), a constant star formation rate of 5  $M_{\odot}$  yr<sup>-1</sup> in the galaxy is taken. We can estimate that there are about  $4.0 \times 10^5$  BeWDs in the galaxy. This estimated number is approximately consistent with the results in Shao & Li (2014). The above uncertainty originates from metallicity. Low metallicity results in a low opacity. Therefore, the stars with low metallicity have radius smaller than those with high metallicity. Long orbital period is unfavorable for the formation of BeWDs and BesdOBs, as shown by Figure 1, which gives the distributions of the initial primary masses and the initial orbital periods for the progenitors of BeWDs, BesdOBs and those binaries in which BesdOBs can evolve into BeWDs.

The initial masses of primaries in the progenitors of BeWDs (the initial masses of WD's progenitors) are between about 2 and  $12~M_{\odot}$ , and mainly are located between about 3 and 8  $M_{\odot}$ . The main reason is that these primaries must transfer enough mass so that their companions can be spun up into Be stars whose masses are higher than 3  $M_{\odot}$ , and themselves can evolve into WDs. The initial orbital periods of BeWDs' progenitors mainly distribute three zones noted by two gaps around  $\sim P_{\rm orb}^{\rm i} = 10^3$  and  $10^2$  days. The binary systems in which  $P_{\rm orb}^{\rm i} > \sim 10^3$  days undergo CEE when the primaries evolve into AGB, those in which  $10^2 < P_{\rm orb}^{\rm i} < \sim 10^3$  days do it when the primaries evolve into Hertzsprung gap or FGB, while those

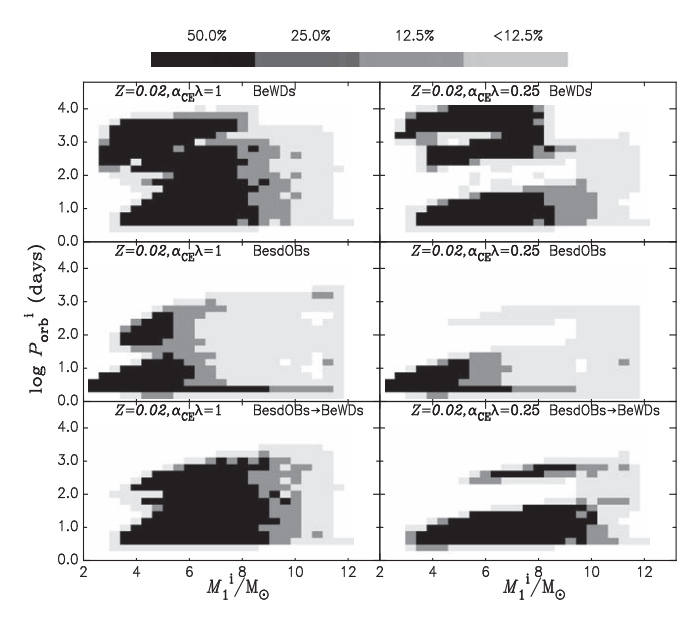


**Figure 2.** Similar to Figure 1, but for the different  $\alpha_{CE} \times \lambda$  during CEE.

with  $P_{\rm orb}^{\rm i} < \sim 10^2$  days undergo stable mass transfer when the primaries fill their Roche lobes during the MS phase. These progenitors with  $P_{\rm orb}^{\rm i} < \sim 10^2$  days first turn into BesdOBs, and then evolve into BeWDs. Another ranges from hundreds to thousands of day. The detailed evolution appears in the third subsection.

Besides the metallicity, CEE also has great effects on the BeWDs. In this work, we calculate the effects of combining parameter  $\lambda \times \alpha_{\rm CE}$  on BeWD and BesdOB binaries. The  $\lambda \times \alpha_{\rm CE}$  is taken as 0.25, 0.5 and 1.0 in the models with Z=0.02, respectively. We find that the fraction of the binary systems evolving into BeWD are 3.5%, 4.1% and 4.6%. The larger  $\lambda \times \alpha_{\rm CE}$  is, the more easily the CE is ejected, that is, binary systems just forming WD can more easily survive after CEE. Combining Figures 1 and 2, CEE mainly affects the evolution of binary systems in which  $10^2 < P_{\rm orb}^{\rm i} < \sim 10^3$  days. As mentioned in the last paragraph, these binary systems can undergo CEE. When  $\lambda \times \alpha_{\rm CE}$  is small, the binary systems hardly survive because the proportion of orbital energy used to eject CE is too small. Therefore, these binary systems cannot evolve into BeWDs when  $\lambda \times \alpha_{\rm CE} = 0.25$ .

Compared with the BeWD progenitors, those of BesdOBs have shallower distribution of the initial orbital periods because the primaries must lose their H-rich envelope before the He in the core is exhausted; they have wider distribution of the initial primary masses because sdOBs can evolve into NSs or even black holes. As Figure 3 shows, the initial masses of secondaries have a similar distribution.

As the important progenitors of BeWDs, BesdOBs also are very interesting. Figure 4 shows the distributions of sdOB masses and Be star masses with the orbital periods in BesdOBs.

In our simulations, there are two peaks for the distribution of orbital periods. One is at about 3 days, and these BeWDs have undergone CEE. Another is at about 40 days, and most of them have undergone the stable mass transfer via Roche lobe. In the galaxy, there are about 11 known BesdOBs or candidates whose orbital periods are observed. As Figure 4 shown, these known BesdOBs and candidates are covered by simulated BesdOBs with long orbital periods. On the observations, there is lack of BesdOBs with the orbital periods between about 2 and 10 days. One main reason is that the orbital periods are too short so that Be stars soon fill their Roche lobes and BesdOBs undergo the second CEE. Another is that Be disk hardly form within so short orbital periods. Theoretically, the He star with a mass higher than about 1.7  $M_{\odot}$  finally evolves into an NS or a black hole (e.g., Hurley et al. 2000). Except  $\chi$  Oph, the masses of sdOBs in 11 known BesdOBs are lower than about 1.7  $M_{\odot}$ , and they have orbital periods longer than about 28 days. Therefore, these BesdOBs will become BeWDs. In our simulations, about 25% of BesdOBs have massive He stars with a mass higher than 1.7  $M_{\odot}$ . They can evolve into Be/Xray binaries if the binaries can survive after a supernova. If the Be star companion in  $\chi$  Oph is an sdOB star, and its mass is about 3.8  $M_{\odot}$  (Harmanec 1987),  $\chi$  Oph may evolve into a Be/ X-ray binary.

Figure 5 gives HR diagrams of Be stars and sdOBs in BesdOBs. Be stars in the known BesdOBs are covered very well by our simulations with high metallicity. However, most of the sdOBs are located at region where the possibility of forming BesdOBs is very low, especially HR 6819 and ALS 8775. The main reason is that the luminosity and the effective temperature in our models only depend on the mass of He star and evolutionary time (Hurley et al. 2000), which results in a shallow region in HR diagram. HR 6819 is a very intriguing object. Rivinius et al. (2020) suggested that HR 6819 is a triple system which is composed of a close inner binary consisting of a B-type giant plus a black hole and an outer Be star with a wide orbit. However, according to an orbital analysis, Bodensteiner et al. (2020) considered that HR 6819 is a BesdOB, which is supported by a new high-angular resolution observation in Frost et al. (2022). Based on the model of binary evolution, Bodensteiner et al. (2020) suggested that sdOB in HR 6819 just evolves to higher effective temperature after mass transfer via Roche lobe, and HR 6819 is very rare. Similarly, ALS 8775, also called as LB-1, was considered as a binary consisting of a B-type star in a 79 day orbit with an about 70  $M_{\odot}$  black hole (Liu et al. 2019). However, Shenar et al. (2020) suggested that ALS 8775 comprises a Be star and a stripped star, that is, it is a BesdOB. Compared with sdOBs in other known BesdOBs, sdOBs in HR 6819 and ALS 8775 have very low effective temperatures. As mentioned in Bodensteiner et al. (2020), these sdOBs just lose their hydrogen-rich envelope, and are evolving into higher effective temperature. Their results are consistent with ours.

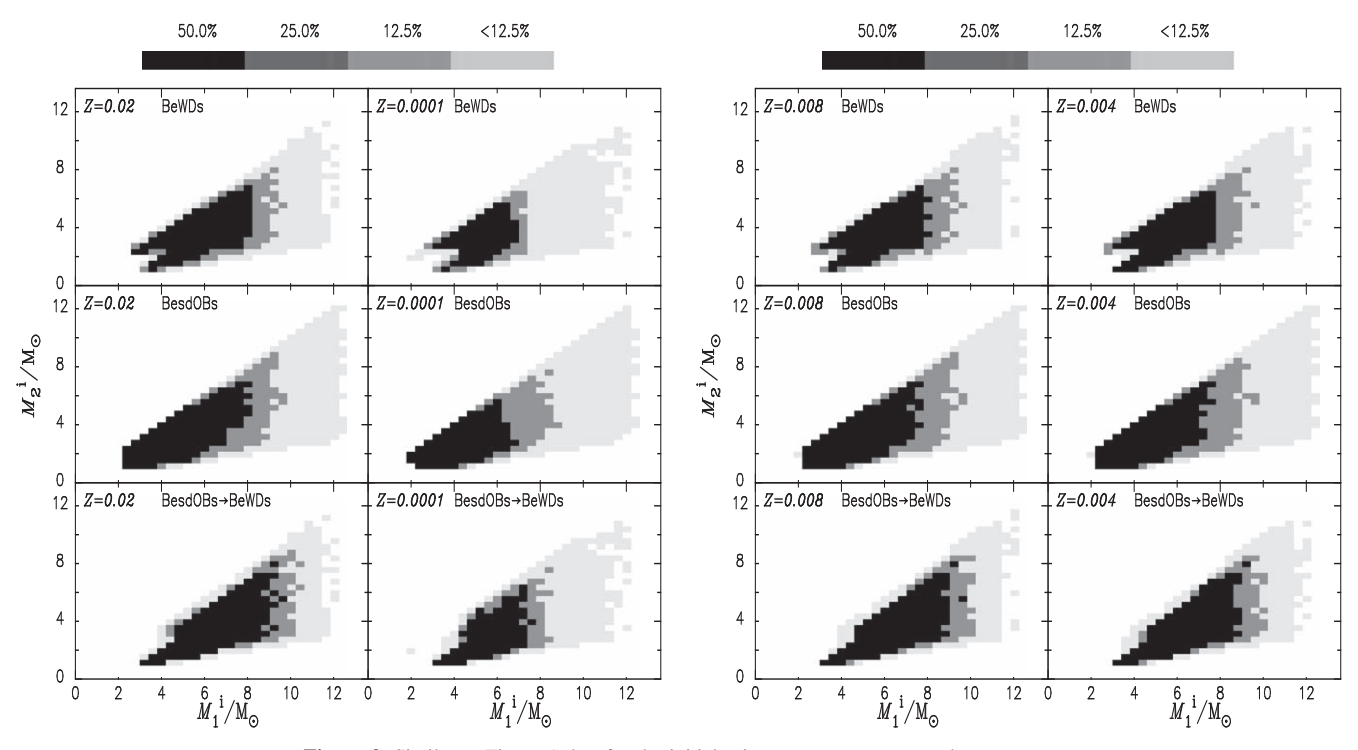


Figure 3. Similar to Figure 1, but for the initial primary masses vs. secondary masses.

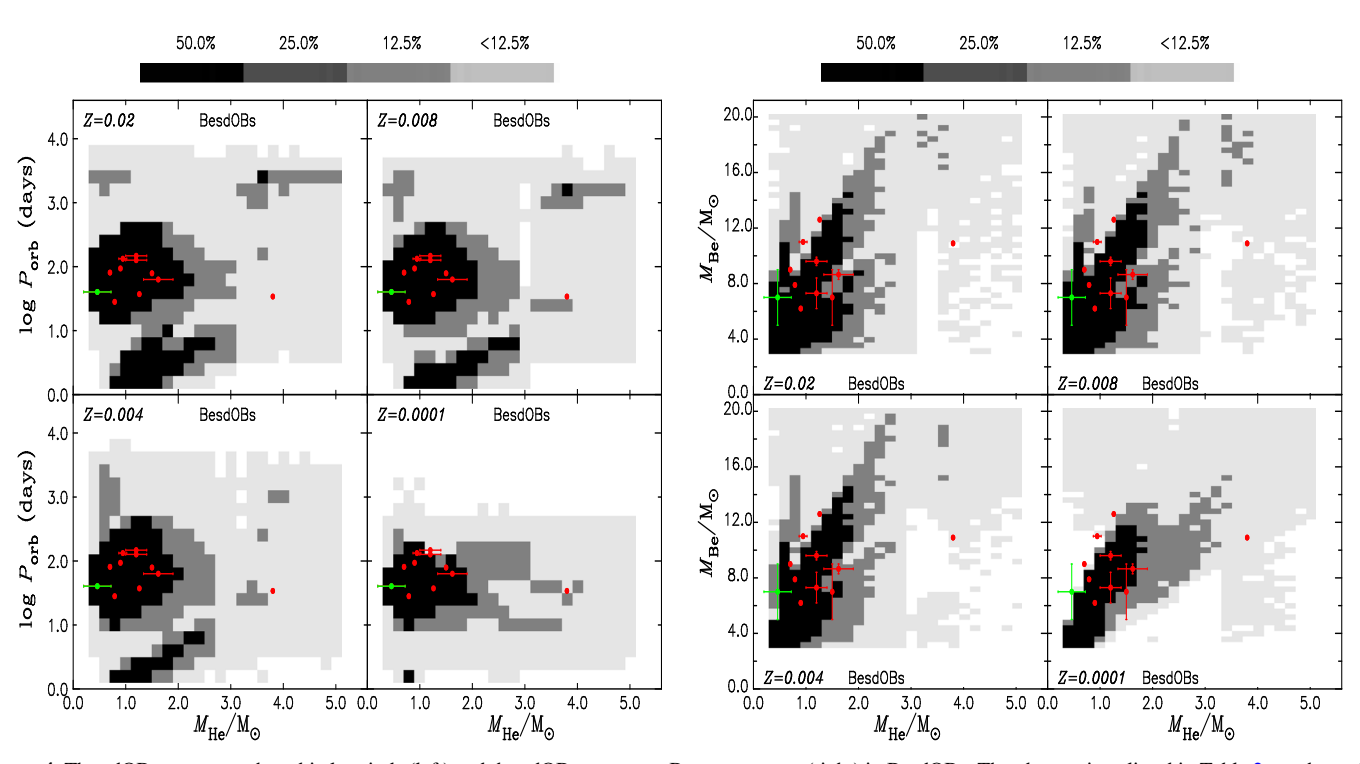


Figure 4. The sdOB masses vs. the orbital periods (left) and the sdOB masses vs. Be stars masses (right) in BesdOBs. The observations listed in Table 2 are shown by red points, and HR 6819 is given by the green point (see text).

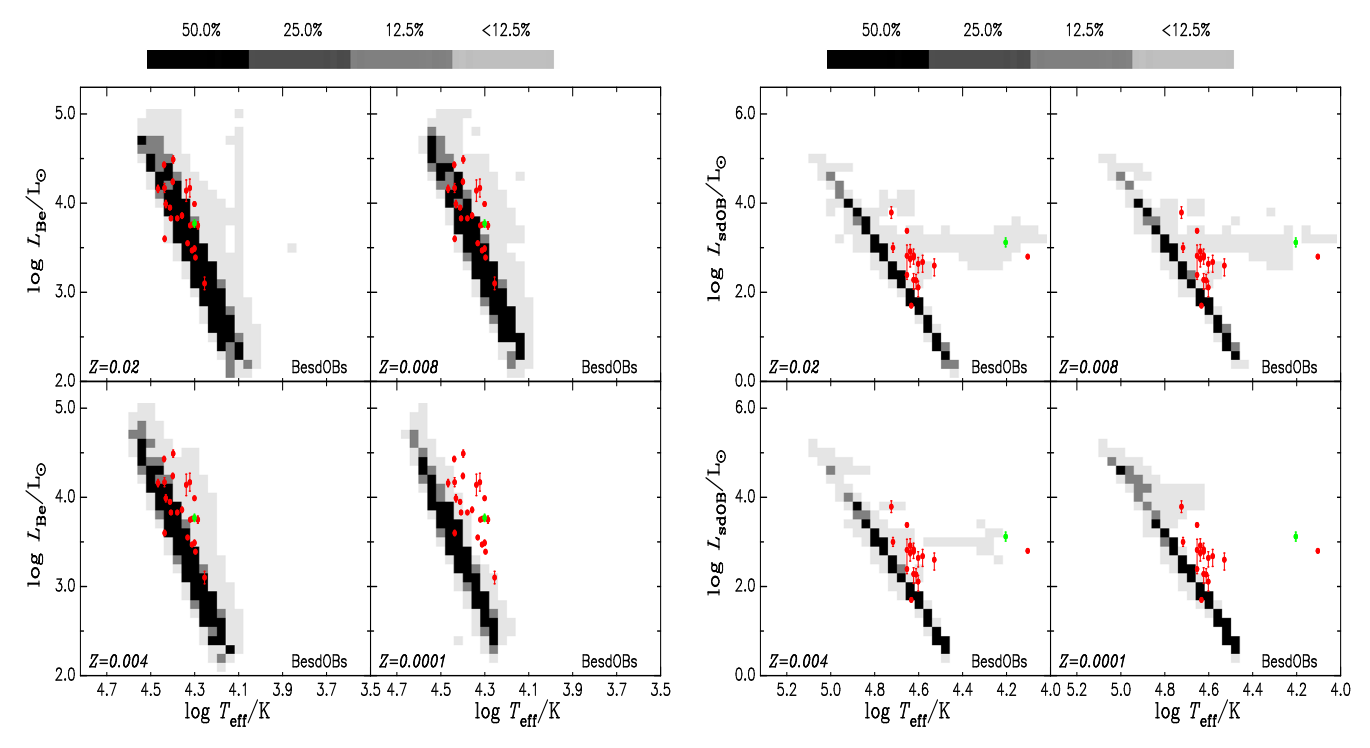
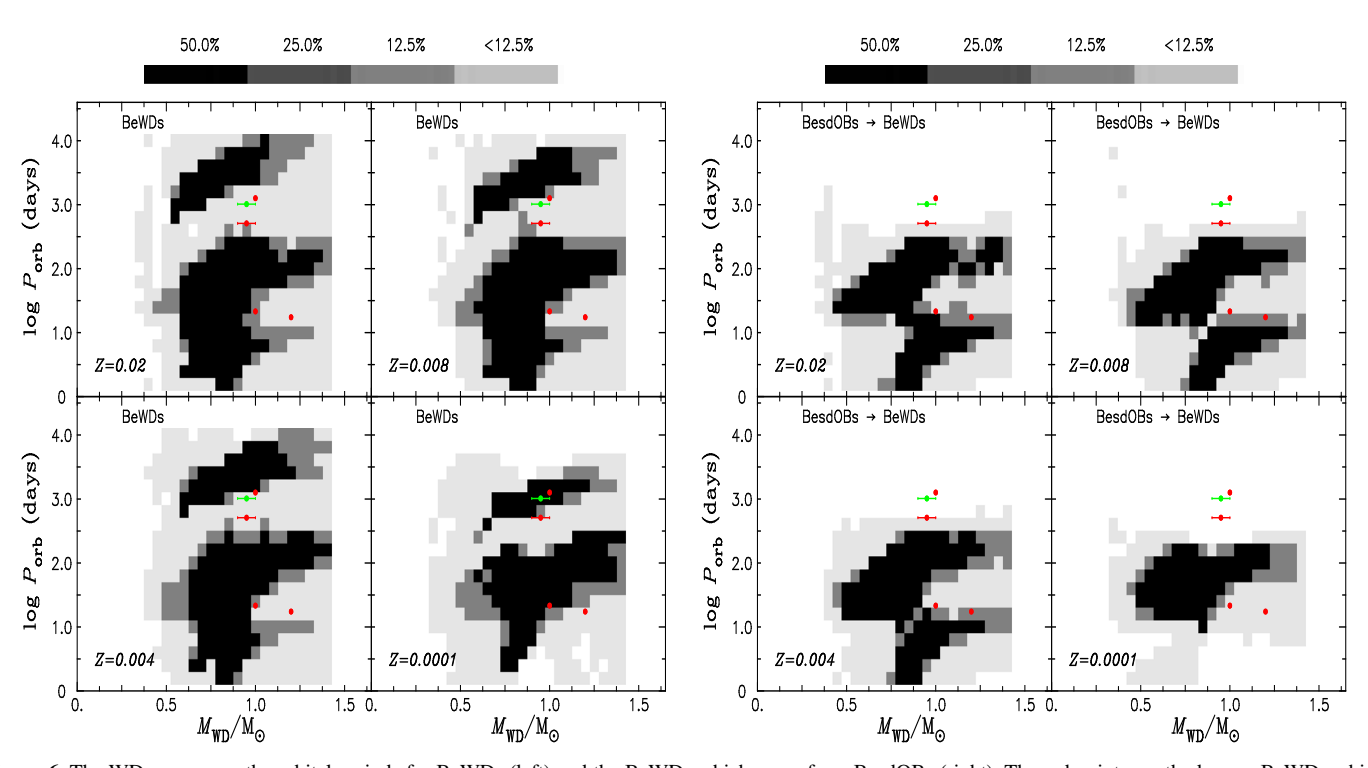


Figure 5. Similar to Figure 4, but for HR diagrams of Be stars (left) and sdOBs (right) in BesdOBs.



**Figure 6.** The WD masses vs. the orbital periods for BeWDs (left) and the BeWDs which come from BesdOBs (right). The red points are the known BeWDs which are listed in Table 1. On observations, the orbital period of XMMU J052016.0-692505 is uncertain, and it has two possible values. The longer orbital period (1020 days) is given by the green point.

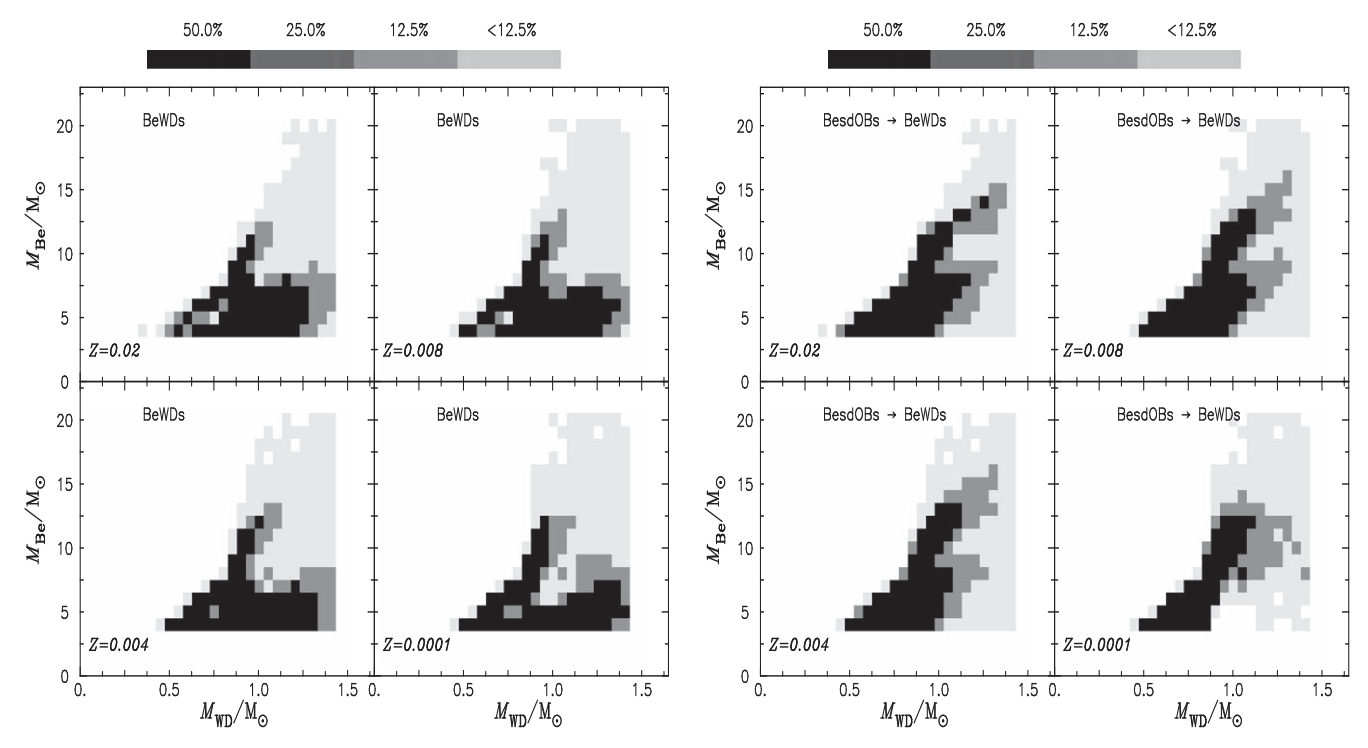


Figure 7. Similar to Figure 6, but for the masses of WDs Be stars in BeWDs.

# 3.2. BeWD Population

All six known BeWDs are detected in the MCs. Considering that metallicity in a galaxy is not well-distributed, we plot BeWDs in all simulations with different metallicities. As illustrated in Figure 6, our results can cover well four BeWDs with known WD's mass and orbital period. The BeWDs with orbital periods shorter than about 300 days (such as SWIFT J011511.0-725611 and J004427.3734801) have undergone the BesdOB phase, while the left BeWDs (such as XMMU J052016.0-692505 and J010147-715550) experience a CEE until their primaries evolve into asymptotic giant branch.

A similar result appears in Figure 7 which shows the distributions of WDs' and Be stars' masses in BeWDs. Obviously, the mass distribution has two zones. One zone has larger q ( $q = M_{\rm Be}/M_{\rm WD}$ ). These BeWDs have undergone efficient mass transfer, and BesdOBs can be their progenitors. Another has low q. These BeWDs have undergone inefficient mass transfer.

Observationally, it is difficult to find a BeWD. The optical properties of BeWDs are similar to those of binaries consisting of Be star and neutron star, and it is hard to distinguish them (Coe et al. 2020). Compared with neutron star X-ray binaries, BeWDs have a soft X-ray range. Usually, if the mass-accretion rate is higher than the minimum stable burning rate ( $M_{\rm cr} \sim 10^{-7}$   $M_{\odot} \, {\rm yr}^{-1}$ ), the accreting WD is a persistent soft X-ray source, or else it is a transient X-ray source during nova burst. For a

persistent soft X-ray source or ones during nova burst, the X-ray luminosity can be estimated by the nuclear burning rate of accreted material (e.g., Wolf et al. 2013; Chen et al. 2015). During the quiet phase, the X-ray emission mainly is produced by the gravitational potential released by material accreted. All known BeWDs are transient X-ray sources. Most of time, they are in the quiet phase. Following Chen (2022), although soft X-ray emission can be easily absorbed by the interstellar medium, the X-ray luminosity of BeWDs can be estimated by the mass-accreting rate via

$$L_{\rm X} = \frac{GM_{\rm WD}}{R_{\rm WD}}\dot{M},\tag{3}$$

where G is gravitational constant.

Figure 8 gives the estimated X-ray luminosities with different  $f_{\rm W}$  s. For the models with  $f_{\rm W}=0$  (a spherical stellar wind, the right sub-figure of Figure 8), our results hardly cover the observational samples. Even for the standard models with  $f_{\rm W}=0.9$  (a decretion disk being dominated in the stellar wind, the left sub-figure of Figure 8), the known BeWDs appear in the top region. There are two possible reasons as follows. One is that our models underestimate the mass-loss rate of Be stars. Carciofi et al. (2012) suggested that the mass-loss rate by decretion disk can reach up to about  $10^{-7}$ – $10^{-10}M_{\odot}$  yr<sup>-1</sup> (Also see Ghoreyshi et al. 2018; Rímulo et al. 2018), which is higher than times of that observed in B stars (Puls et al. 2008). Another is that these BeWDs measured X-ray luminosities are

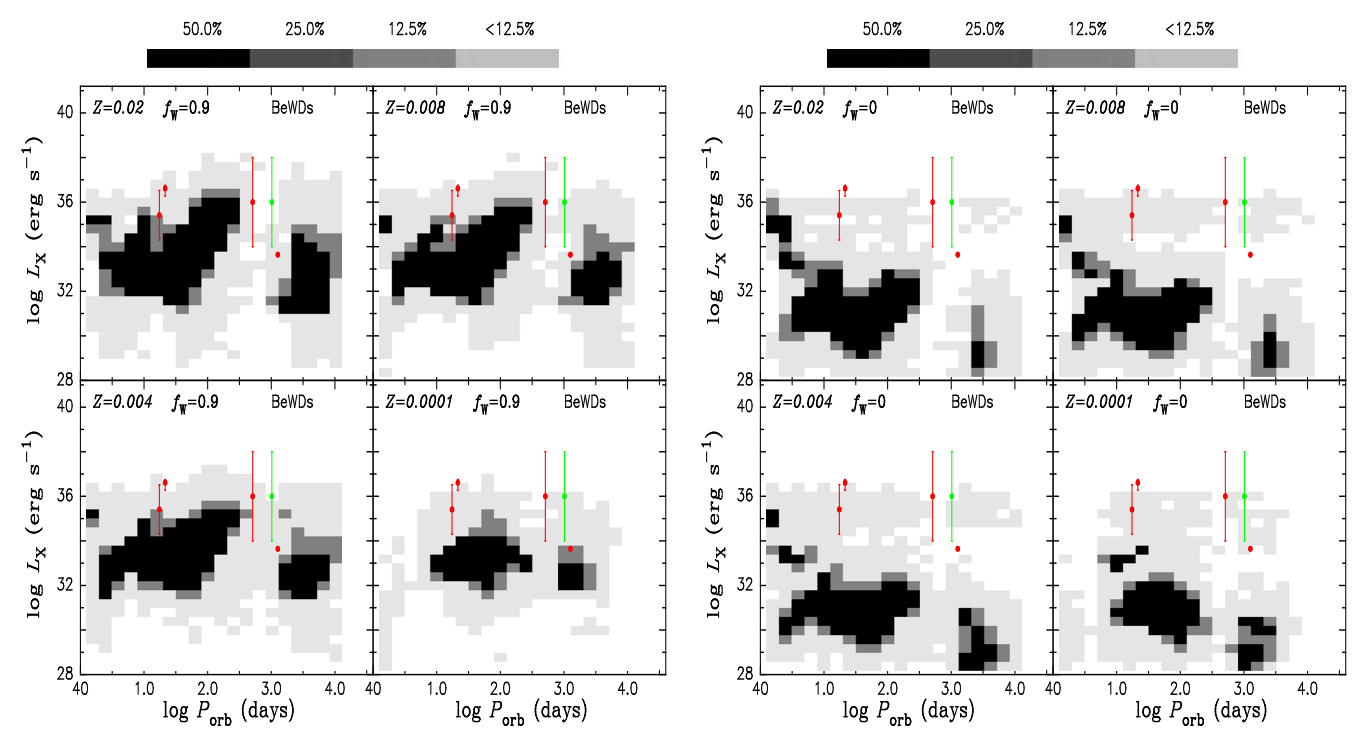


Figure 8. Similar to Figure 6, but for the orbital periods vs. X-ray luminosities calculated by Equation (3). The left and the right sub-figures represent the simulations of  $f_W = 0.9$  and 0, respectively.

on the outburst phase. In BeWDs, outbursts are divided into two types. The type-I outburst originates from the thermonuclear runaway (TNR). Usually, the X-ray luminosity produced by TNR in BeWDs is too faint to be detected. The type-II outburst is triggered by accretion-disk instability. SWIFT J011511.0-725611 just experienced a type-II outburst (Kennea et al. 2021). The X-ray luminosity during the type-II outburst can be higher than that during the quiet phase for at least two orders of magnitude (Kahabka et al. 2006; Kennea et al. 2021). Therefore, the model with a stellar wind dominated by decretion disk is better.

# 3.3. BeWD Destiny

Theoretically, BeWD destiny depends on not only its orbital period and mass ratio ( $q=\frac{M_{\rm Be}}{M_{\rm WD}}$ ), but also WD types (CO or ONe WD). In our simulations, the ratios of COWDs to ONeWDs in BeWDs are about 7/3 (Z=0.02) and 6/4 (Z=0.0001). This ratio is mainly determined by the initial mass forming CO and ONe WDs. The former range of initial masses in BeWDs is between about 2 and 6  $M_{\odot}$ , while the later is between about 6 and 12  $M_{\odot}$ .

Figure 9 shows the distributions of the orbital periods and q for BeCOWDs and BeONeWDs. There are four zones which are noted "A," "B," "C" and "D." Every zone represents different evolutionary channels. The proportions of BeCOWDs produced by A, B, C and D channels are about 20%, 35%, 25%

and 20% in all simulations except that they are about 5%, 50%, 35% and 10% in the extremely metal-poor simulation (Z = 0.0001). For BeONeWDs, they are about 40%, 20%, 20% and 20% in the metal-rich models, while they are about 0, 50%, 30% and 25% in the extremely metal-poor simulation.

As mentioned in subsection 3.1, BeWDs in A and B zones have been BesdOBs. Differently, the progenitors of BeCOWDs (or BeONeWDs) in A zone have orbital periods whose range is between about 20 (30) and 200 (600) days. Their primaries fill their Roche lobes on the late phase of Hertzsprung gap or even giant phase. When they evolve into the first giant branch, the progenitors experience CEE. If the binaries do not merge, the orbital periods shrink to about several percents, the primaries become sdOBs, and the secondaries are spun up to Be stars via mass accretion before CEE or tidal interaction after CEE. The progenitors become BesdOBs, and then they evolve into BeWDs with the shortest orbital periods. The progenitors of BeCOWDs (or BeONeWDs) in B zone have initial orbital periods shorter than 20 (30) days. Their progenitors fill Roche lobes during main sequence, and undergo a stable and efficient mass transfer so that the secondary masses exceed primary ones. Even the primaries evolve into the first giant branch, the mass transfer is still stable, which results in lengthening orbital periods. For the BeWDs in C and D zones, their progenitors have wide orbits. The progenitors of BeCOWDs (or BeO-NeWDs) in C zone have the orbital periods between about 200

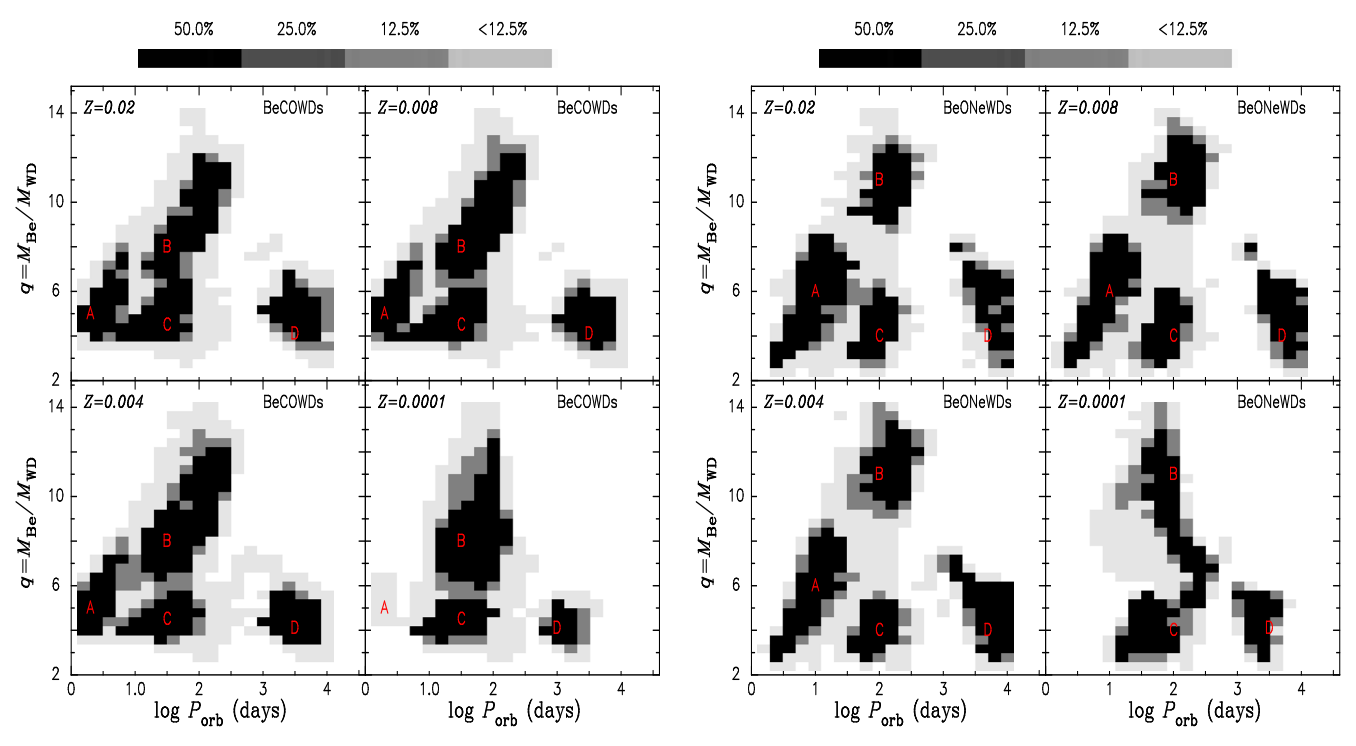


Figure 9. Distributions of the orbital periods vs. the  $q(q = \frac{M_{\text{Be}}}{M_{\text{WD}}})$  for BeCOWDs (left) and BeONeWDs (right). The letters "A," "B," "C" and "D" represent different evolutionary channels (see text).

(600) and 1000 (2000) days, their primaries fill Roche lobes until they evolve into early AGB phase. Usually, these binaries undergo CEE. For the BeWDs in D zone, the orbital periods of their progenitors are so long that the primaries cannot fill Roche lobes. The secondaries are spun via accreting stellar wind. For very metal-poor models (Z = 0.0001), A zone lacks BeWDs. The main reason is as follows: very low metallicity results in very small stellar radius so that the primaries cannot fill their Roche lobe.

### 3.3.1. Merger of WD and Non Degenerated Star

Be stars or their successors in BeWDs in the A, B and C zones of Figure 9 can fill their Roche lobes with their evolution. If q is higher than  $q_{\rm cr}$ , CEE occurs. It is well known that CEE can produce two different results: merger if the CE cannot be ejected, or else a close binary. The former is usually occurs when Be stars or their successors are on main sequence or Hertzsprung gap, which is a merger of WD and H-rich star. The later usually forms the close binary consisting of a WD and a He star. With He star evolution, it also fills its Roche lobe. CEE may occur again, which produces a merger of a WD and a He star or double WDs.

Figure 10 shows the mass distributions of stars produced by merger of a WD and a non degenerated star. Here, we do not consider the mass loss during merger events. In our

simulations, about 60% (Z=0.02) -70% (Z=0.0001) of BeWDs finally merge into single star systems, in which about 80% (Z=0.02) -90% (Z=0.0001) of merger events involve WD and H-rich star. These mergers may observationally correspond to luminous red novae (Soker & Tylenda 2003; Ivanova et al. 2013; Howitt et al. 2020). The left mergers involving WD and He-rich star may form He giant stars (e.g., Hurley et al. 2002). Their progenitors have successfully experienced CEE, and the envelope of Be stars or their successors are ejected. Therefore, the mass of these He giant stars is lower than about  $2.0~M_{\odot}$ .

# 3.3.2. Double White Dwarf Binaries

About 30%–40% of BeWDs' successors do not merge during CEEs. They usually evolve into double WDs. They represent the most likely gravitational wave source (GWS) detected by the LISA mission (e.g. Amaro-Seoane et al. 2017). Peters & Mathews (1963) gave the GW luminosity of a binary system. Assuming an orbital period and a sinusoidal wave, the strain amplitude of GW, h, can be given by

$$h = 5.0 \times 10^{-22} \left(\frac{\mathcal{M}}{M_{\odot}}\right)^{5/4} \left(\frac{P_{\text{orb}}}{1 \text{hr}}\right)^{-2/3} \left(\frac{d}{1 \text{kpc}}\right)^{-1},$$
 (4)

where  $\mathcal{M} = (M_1 M_2)^{3/5}/(M_1 + M_2)^{1/5}$  is the chirp mass. Considering that the distances of most double WDs known in

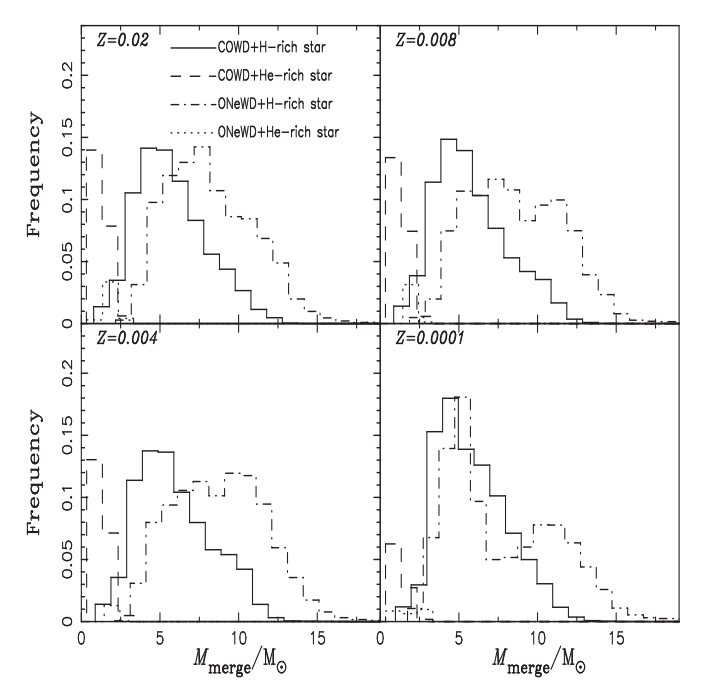


**Figure 10.** Mass distributions of stars produced by merger of a WD and a non degenerated star. Different lines represent the merger of different types of WD and star, which are given in the top-middle zone. The frequency of mergers involving COWDs and ONeWDs is normalized to 1, respectively.

the galaxy is shorter than 1 kpc (Korol et al. 2017; Kupfer et al. 2018; Burdge et al. 2019; Li et al. 2020), we take d as 1 kpc. Figure 11 gives the distribution of GWs from double WDs in the strain-frequency space. The GWs' frequency detected potentially by LISA are mainly at about  $3 \times 10^{-3}$  and  $\times 10^{-2}$  Hz, which greatly depends on the LISA sensitivity.

# 3.4. Supernova Ia Progenitors

Following Lü et al. (2009), we also structure an aspherical stellar-wind model for BeWDs. It depends on the mass-accretion rates ( $\dot{M}_{\rm a}$ ) whether an accreting WD's mass can efficiently increase (e.g., Nomoto et al. 2007). If  $\dot{M}_{\rm a}$  is higher than a critical value ( $\dot{M}_{\rm cr}$ ), the accreted hydrogen materials can steadily burn, or less TNR can occur on the surface of accreting WD. For the former, the accreted materials can efficiently turn into WD matter after the burning. For the later, the accreted materials can partly be ejected during the TNR, even WD matter is eroded when  $\dot{M}_{\rm a}$  is lower than about  $\frac{1}{8}\dot{M}_{\rm cr}$  (Yaron et al. 2005; Lü et al. 2006)

Figure 12 shows the distribution of WD's mass and mass-accretion rate in BeWDs. Obviously, the mass-accretion rates of WDs in BeWDs almost are lower than  $\dot{M}_{\rm cr}$ , and the majority of them are lower than  $\frac{1}{8}\dot{M}_{\rm cr}$ . Therefore, in our simulations, there is not a sample in which COWD's mass can reach up to

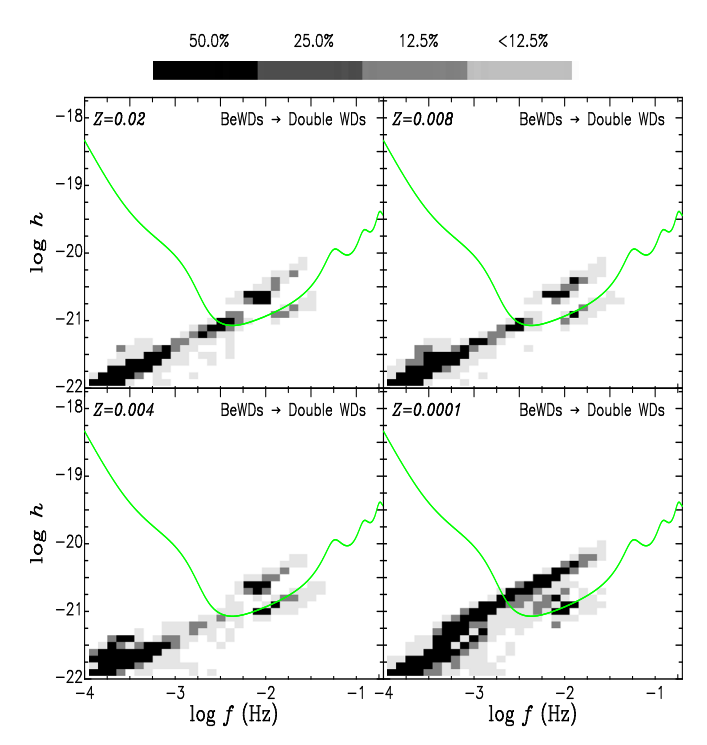


Figure 11. Distribution of gravitational sources from double WDs in the strain-frequency space. Green lines give the LISA sensitivity.

 $1.35~M_{\odot}$  and ONeWD's mass can reach up to  $1.44~M_{\odot}$  in BeWDs. Therefore, BeWDs hardly occur SN Ia.

### 4. Conclusions

Using the method of population synthesis, we investigate the formation and the destiny of BeWDs. The effects of the metallicity and the combining parameters  $\lambda \times \alpha_{\rm CE}$  of CEE on BeWD population are discussed. For  $\lambda \times \alpha_{CE} = 0.5$ , about 3.7% (Z = 0.0001)-4.1% (Z = 0.02) of binary systems can evolve into BeWDs; about 60% (Z = 0.0001)-70% (Z = 0.02) of BeWDs include a COWD, and 30%-40% of them have an ONeWD; about 40% (Z = 0.0001) -45% (Z = 0.02) of BeCOWDs have undergone CEE, about 35% (Z = 0.0001) -50% (Z = 0.02) of them have experienced heavy mass transfer, and about 10% (Z = 0.0001) -20% (Z = 0.02) of them exchange materials via stellar winds; for BeONeWDs, the above proportions are 50%-60%, 20%-30% and 20%-30%, respectively. Changing the combining parameter  $\lambda \times \alpha_{CE}$  from 0.25 to 0.5, it introduces an uncertainty with a factor of about 1.3 on BeWD populations. It mainly affects BeWDs which are formed via CEE of the binary systems with  $10^2 < P_{\rm orb}^{\rm i} < \sim 10^3 \text{ days.}$ 

About 30%–50% of BeWDs come from BesdOBs which are important progenitors. Our results can cover well the observational properties of BesdOBs' population, including rare sources: HR 6819 and ALS 8775. BesdOBs mainly evolve

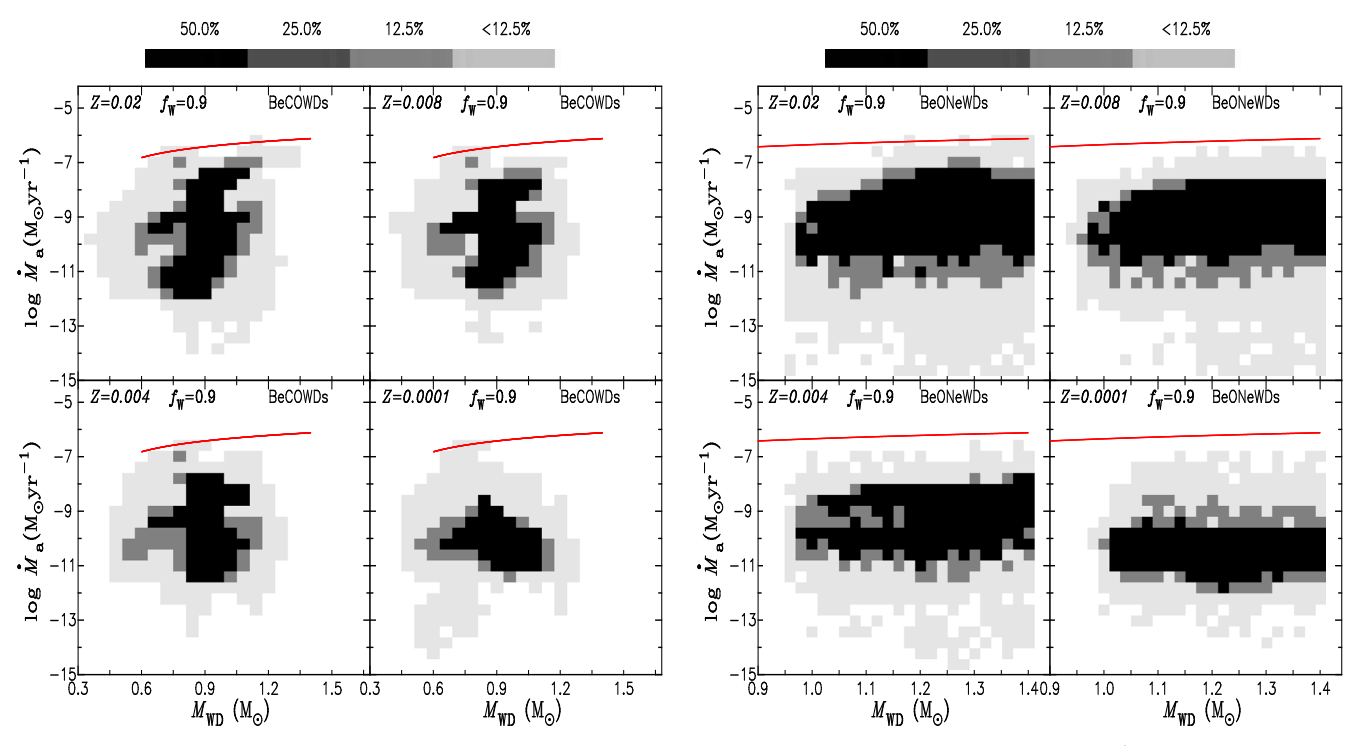


Figure 12. Distributions of WD mass vs. the mass-accretion rates in BeWDs. Red lines represent the critical mass-accretion rate ( $\dot{M}_{cr}$ ) for the accreted hydrogen burning steadily on the surface of the WD.

into the BeWDs with orbital periods shorter than about 300 days. About 60%–70% of BeWDs occur a merger between a WD and a non-degenerated star in which 90% are H-rich stars and the left are He stars. About 30%–40% of BeWDs turn into double WDs which are potential GWs of the LISA mission at a frequency band between about  $3\times10^{-3}$  and  $\times10^{-2}$  Hz. Due to a low mass-accretion rate of WD, BeWDs hardly become the progenitors of SN Ia.

One should note that the uncertainties of BPS in our work only result from the metallicity and the CEE. It is well known that many input parameters (accretion efficiency during mass transfer, the criteria of dynamical mass transfer, etc.) can affect the results of BPS. If the effects of the combining parameters are considered, the uncertainties of BPS should be larger.

# Acknowledgments

This work received the generous support of the Natural Science Foundation of Xinjiang No. 2021D01C075; the National Natural Science Foundation of China, project Nos. 12163005, U2031204 and 11863005; the science research grants from the China Manned Space Project with No. CMS-CSST-2021-A10.

# References

Ablimit, I., & Lü, G. 2013, SCPMA, 56, 663 Abt, H. A., & Levy, S. G. 1978, ApJS, 36, 241

```
Bjorkman, J. E., & Cassinelli, J. P. 1993, ApJ, 409, 429
Bodensteiner, J., Shenar, T., Mahy, L., et al. 2020, A&A, 641, A43
Bogovalov, S., & Petrov, M. 2021, Universe, 7, 353
Bondi, H., & Hoyle, F. 1944, MNRAS, 104, 273
Brown, R. O., Coe, M. J., Ho, W. C. G., et al. 2019, MNRAS, 488, 387
Burdge, K. B., Coughlin, M. W., Fuller, J., et al. 2019, Natur, 571, 528
Carciofi, A. C., Bjorkman, J. E., Otero, S. A., et al. 2012, ApJL, 744, L15
Carrier, F., Burki, G., & Burnet, M. 2002, A&A, 385, 488
Chen, H.-L., Woods, T. E., Yungelson, L. R., et al. 2015, MNRAS, 453, 3024
Chen, W.-C. 2022, A&A, 662, A79
Chojnowski, S. D., Labadie-Bartz, J., Rivinius, T., et al. 2018, ApJ, 865, 76
Coe, M. J., Kennea, J. A., Evans, P. A., et al. 2020, MNRAS, 497, L50
D'Antona, F., & Tailo, M. 2020, arXiv:2011.11385
de Mink, S. E., Langer, N., Izzard, R. G., et al. 2013, ApJ, 764, 166
Ekström, S., Meynet, G., Maeder, A., et al. 2008, A&A, 478, 467
Frost, A. J., Bodensteiner, J., Rivinius, T., et al. 2022, A&A, 659, L3
Ghoreyshi, M. R., Carciofi, A. C., Rímulo, L. R., et al. 2018, MNRAS,
  479, 2214
Han, Z., Podsiadlowski, P., Maxted, P. F. L., et al. 2002, MNRAS, 336, 449
Han, Z.-W., Ge, H.-W., Chen, X.-F., et al. 2020, RAA, 20, 161
Harmanec, P. 1987, Bull. Astron. Inst. Czech., 38, 283
Hastings, B., Langer, N., Wang, C., et al. 2021, A&A, 653, A144
Haubois, X., Carciofi, A. C., Rivinius, T., et al. 2012, ApJ, 756, 156
Heber, U. 1986, A&A, 155, 33
Howitt, G., Stevenson, S., Vigna-Gómez, A., et al. 2020, MNRAS, 492, 3229
Hurley, J. R., Pols, O. R., & Tout, C. A. 2000, MNRAS, 315, 543
Hurley, J. R., Tout, C. A., & Pols, O. R. 2002, MNRAS, 329, 897
Ivanova, N., Justham, S., Avendano Nandez, J. L., et al. 2013, Science,
  339, 433
Kahabka, P., Haberl, F., Payne, J. L., et al. 2006, A&A, 458, 285
Kennea, J. A., Coe, M. J., Evans, P. A., et al. 2021, MNRAS, 508, 781
Kiel, P. D., & Hurley, J. R. 2006, MNRAS, 369, 1152
Klement, R., Schaefer, G. H., Gies, D. R., et al. 2022, ApJ, 926, 213
Korol, V., Rossi, E. M., Groot, P. J., et al. 2017, MNRAS, 470, 1894
```

Amaro-Seoane, P., Audley, H., Babak, S., et al. 2017, arXiv:1702.00786

```
Koubský, P., Kotková, L., Kraus, M., et al. 2014, A&A, 567, A57
Koubský, P., Kotková, L., Votruba, V., et al. 2012, A&A, 545, A121
Kupfer, T., Korol, V., Shah, S., et al. 2018, MNRAS, 480, 302
Langer, N. 1998, A&A, 329, 551
Li, K. L., Kong, A. K. H., Charles, P. A., et al. 2012, ApJ, 761, 99
Li, Z., Chen, X., Chen, H.-L., et al. 2020, ApJ, 893, 2
Liu, J., Zhang, H., Howard, A. W., et al. 2019, Natur, 575, 618
Liu, Q. Z., van Paradijs, J., & van den Heuvel, E. P. J. 2005, A&A, 442, 1135
Liu, Q. Z., van Paradijs, J., & van den Heuvel, E. P. J. 2006, A&A, 455, 1165
Lü, G., Yungelson, L., & Han, Z. 2006, MNRAS, 372, 1389
Lü, G., Zhu, C., & Podsiadlowski, P. 2013, ApJ, 768, 193
Lü, G., Zhu, C., Wang, Z., et al. 2009, MNRAS, 396, 1086
Lü, G., Zhu, C., Wang, Z., et al. 2020, ApJ, 890, 69
Lü, G.-L., Zhu, C.-H., Postnov, K. A., et al. 2012, MNRAS, 424, 2265
Meurs, E. J. A., & van den Heuvel, E. P. J. 1989, A&A, 226, 88
Miller, G. E., & Scalo, J. M. 1979, ApJS, 41, 513
Morii, M., Tomida, H., Kimura, M., et al. 2013, ApJ, 779, 118
Mourard, D., Monnier, J. D., Meilland, A., et al. 2015, A&A, 577, A51
Naze, Y., Rauw, G., Smith, M. A., et al. 2022, arXiv:2208.03990
Nomoto, K., Saio, H., Kato, M., et al. 2007, ApJ, 663, 1269
Oliveira, A. S., Steiner, J. E., Ricci, T. V., et al. 2010, A&A, 517, L5
Panoglou, D., Carciofi, A. C., Vieira, R. G., et al. 2016, MNRAS, 461, 2616 Peters, G. J., Pewett, T. D., Gies, D. R., et al. 2013, ApJ, 765, 2
Peters, G. J., Wang, L., Gies, D. R., et al. 2016, ApJ, 828, 47
Peters, P. C., & Mathews, J. 1963, PhRv, 131, 435
```

```
Porter, J. M., & Rivinius, T. 2003, PASP, 115, 1153
Puls, J., Vink, J. S., & Najarro, F. 2008, A&ARv, 16, 209
Raguzova, N. V. 2001, A&A, 367, 848
Rímulo, L. R., Carciofi, A. C., Vieira, R. G., et al. 2018, MNRAS, 476, 3555
Rivinius, T., Baade, D., Hadrava, P., et al. 2020, A&A, 637, L3
Rivinius, T., Carciofi, A. C., & Martayan, C. 2013, A&ARv, 21, 69
Ruždjak, D., Božić, H., Harmanec, P., et al. 2009, A&A, 506, 1319
Sargent, W. L. W., & Searle, L. 1968, ApJ, 152, 443
Shao, Y., & Li, X.-D. 2014, ApJ, 796, 37
Shao, Y., & Li, X.-D. 2021, ApJ, 908, 67
Shenar, T., Bodensteiner, J., Abdul-Masih, M., et al. 2020, A&A, 639, L6
Soker, N., & Tylenda, R. 2003, ApJL, 582, L105
Sturm, R., Haberl, F., Pietsch, W., et al. 2012, A&A, 537, A76
Tycner, C., Jones, C. E., Sigut, T. A. A., et al. 2008, ApJ, 689, 461
Vieira, R. G., Carciofi, A. C., Bjorkman, J. E., et al. 2017, MNRAS, 464, 3071
Vink, J. S., de Koter, A., & Lamers, H. J. G. L. M. 2000, A&A, 362, 295
Vink, J. S., de Koter, A., & Lamers, H. J. G. L. M. 2001, A&A, 369, 574
Wang, B., & Han, Z. 2012, NewAR, 56, 122
Wang, L., Gies, D. R., & Peters, G. J. 2018, ApJ, 853, 156
Wang, L., Gies, D. R., Peters, G. J., et al. 2021, AJ, 161, 248
Wolf, W. M., Bildsten, L., Brooks, J., et al. 2013, ApJ, 777, 136
Yaron, O., Prialnik, D., Shara, M. M., et al. 2005, ApJ, 623, 398
Zhu, C., Liu, H., Lü, G., et al. 2019, MNRAS, 488, 525
Zhu, C., Liu, H., Wang, Z., et al. 2021, A&A, 654, A57
Zhu, C., Lü, G., & Wang, Z. 2015, MNRAS, 454, 1725
```